Designing Coupling for Synchronization and Amplification of Chaos

Ioan Grosu,[1] E. Padmanaban,[2] Prodyot K. Roy,[3] and Syamal K. Dana[2,*]

[1]*Faculty of Bioengineering, University of Medicine and Pharmacy, "Gr. T. Popa," Iasi, Romania*
[2]*Indian Institute of Chemical Biology, Jadavpur, Kolkata 700032, India*
[3]*Department of Physics, Presidency College, Kolkata 700073, India*

(Received 14 April 2008; published 12 June 2008)

We propose a design of coupling for stable synchronization and antisynchronization in chaotic systems under parameter mismatch. The antisynchronization is independent of the specific symmetry (reflection symmetry, axial symmetry, or other) of a dynamical system. In the synchronization regimes, we achieve amplification (attenuation) of a chaotic driver in a response oscillator. Numerical examples of a Lorenz system, Rössler oscillator, and Sprott system are presented. Experimental evidence is shown using an electronic version of the Sprott system.

DOI: 10.1103/PhysRevLett.100.234102 PACS numbers: 05.45.Gg, 05.45.Xt

Applications of chaos synchronization are being explored in secure communication [1] and nano-oscillators [2] and for understanding neurocomputing [3] and cognitive dysfunction in the brain [4], which are based on either complete synchronization (CS) [5] or phase synchronization (PS) [6]. CS is observed in identical systems under strong interactions, yet its stability is susceptible [7] to parameter mismatch and noise. In the presence of parameter mismatch, PS is observed in chaotic systems [6] under weak interactions above a threshold when the amplitudes remain almost uncorrelated. PS can be of the in-phase (zero-phase difference) or the antiphase (π-phase difference) type. A type of antiphase synchronization is antisynchronization (AS) [8–11], where the oscillators have identical amplitudes, too.

Establishing CS or AS in chaotic oscillators under parameter mismatch is a challenging task. But it is important for engineering applications since no two oscillators can be identical in reality. Existing coupling schemes [6,7] failed to preserve the stability of synchronization under parameter mismatch. New coupling strategies need to be formulated to address this issue of stability. We explore, in this Letter, an open-loop–closed-loop (OPCL) based coupling scheme [12] that ensures stable CS and AS in the presence of mismatch.

AS is usually observed [8–10] in reflection symmetric systems that remain invariant under the inversion $(x, y, z) \rightarrow (-x, -y, -z)$ of the state variables, while an axial symmetric system such as a Lorenz oscillator is invariant under a transformation $(x, y, z) \rightarrow (-x, -y, z)$, where only partial AS [9,10] is observed using the conventional linear coupling. In partial AS, some of the state variables are in AS while the others are in CS. On the other hand, in a Rössler oscillator, none of the above symmetries exist, and AS is not observed. By using the OPCL coupling, we provide counterintuitive examples that reveal AS in all such systems without restrictions on the symmetry class of a dynamical system.

Most importantly, in the synchronization regimes, we are able to amplify (attenuate) a chaotic attractor in a response system. Amplification (attenuation) of a chaotic attractor was reported earlier [13] using the master-slave coupling [5]. There the amplification of the chaotic attractor of a Lorenz system was shown in a replica of its subsystem as a response system, when the drive and the response develop a state of uniformly stable synchrony [13]. However, the amplification was uncertain to achieve since it was found to be sensitive to initial conditions and perturbation. In contrast, we realize stable amplification (attenuation) in any coupled chaotic system, identical as well as mismatched, using our proposed coupling. We focus our attention here on AS and amplification using numerical examples of a Lorenz system, a Rössler oscillator, and a Sprott system [14]. We demonstrate a physical realization of the coupling in electronic circuit.

The OPCL coupling was used earlier for CS in identical oscillators [12] and synchronization of identical complex networks [15]. To extend the coupling to mismatch systems, we define a driver $\dot{y} = F(y) + \Delta F(y)$, $y \in R^n$, where $\Delta F(y)$ contains mismatch parameters. It drives a response system $\dot{x} = F(x)$, $x \in R^n$, to achieve a goal dynamics $g(t) = \alpha y(t)$; α is a constant. The driven system is given by

$$\dot{x} = F(x) + D(x, \alpha y), \tag{1}$$

where the coupling $D(x, \alpha y)$ is defined by

$$D(x, \alpha y) = \alpha \dot{y} - F(\alpha y) + [H - JF(\alpha y)](x - \alpha y). \tag{2}$$

$J = \partial/\partial(\alpha y)$ is the Jacobian, and H is an arbitrary constant Hurwitz matrix (nxn) whose eigenvalues all have negative real parts. The error signal of the coupled system is defined by $e = x - \alpha y$, and $F(x)$ can be written, using the Taylor series expansion, by

$$F(x) = F(\alpha y) + JF(\alpha y)(x - \alpha y) + \cdots. \tag{3}$$

Keeping the first order terms in (3) and substituting in (2), the error dynamics is obtained as $\dot{e} = He$ from (1), and this ensures that $e \rightarrow 0$ [12]. When $[JF(\alpha y)]_{ij}$ in (2) is a constant, we choose H_{ij} such that $[H - JF(\alpha y)]_{ij}$ is

zero. However, if $[JF(\alpha y)]_{ij}$ is a variable, we choose $H_{ij} = p_{ij}$. The parameters p_{ij} are chosen to satisfy the Routh-Hurwitz (RH) conditions. For $n = 3$, the characteristic equation of the H matrix is given by $\lambda^3 + a_1\lambda^2 + a_2\lambda + a_3 = 0$, and the corresponding RH conditions are $a_1 > 0$, $a_1a_2\text{-}a_3 > 0$, $a_3 > 0$ [12]. This ensures stability of synchronization even in mismatch oscillators. α can now be used as a control parameter to induce flip-flopping between CS ($\alpha = 1$) and AS ($\alpha = -1$) states, which is of practical use in digital encoding [16].

The coupling scheme is first elaborated by using a numerical example of the Lorenz system

$$\dot{x}_1 = \sigma(x_2 - x_1); \qquad \dot{x}_2 = rx_1 - x_2 - x_1x_3; \qquad \dot{x}_3 = -bx_3 + x_1x_2. \tag{4}$$

We consider another Lorenz system with mismatch

$$\begin{aligned} \dot{y}_1 &= \sigma(y_2 - y_1) + \Delta\sigma(y_2 - y_1); \\ \dot{y}_2 &= ry_1 - y_2 - y_1y_3 + \Delta ry_1; \\ \dot{y}_3 &= -by_3 + y_1y_2 - \Delta by_3, \end{aligned} \tag{5}$$

where $\Delta\sigma$, Δr, and Δb are the mismatches in parameters. The system (5) drives the response (4) for replication or amplification of its dynamics. The coupling is derived by using (2), and then by adding to (4) the driven Lorenz system is

$$\begin{aligned} \dot{x}_1 &= \sigma(x_2 - x_1) + \alpha\Delta\sigma(1/\varepsilon)(y_2 - y_1), \\ \dot{x}_2 &= rx_1 - x_2 - x_1x_3 + \alpha\Delta ry_1 + \alpha(\alpha - 1)y_1y_3 \\ &\quad + (p_1 + \alpha y_3)(x_1 - \alpha y_1) + (p_2 + \alpha y_1)(x_3 - \alpha y_3), \\ \dot{x}_3 &= -bx_3 + x_1x_2 - \alpha\Delta by_3 + \alpha(1 - \alpha)y_1y_2 \\ &\quad + (p_3 - \alpha y_2)(x_1 - \alpha y_1) + (p_4 - \alpha y_1)(x_2 - \alpha y_2). \end{aligned} \tag{6}$$

Clearly, the coupling has nonlinear components with additional linear coupling terms, one for each mismatch. ε is a tuning parameter inserted deliberately in (6) to test how the coupling term due to a mismatch ($\Delta\sigma$) plays an effective role in stabilizing synchronization as elaborated later. Note that $\varepsilon = 1$ for the current simulation. The Hurwitz matrix H (3×3) for the driven Lorenz system is $H = |-\sigma\ \sigma\ 0; r + p_1\ -1\ p_2; p_3\ p_4\ -b|^T$; T denotes transpose of a matrix. The coupling in (6) can be simplified by appropriate choices of p_k $(k = 1, 2, 3, 4)$ in H. A suitable choice is $p_1 < 1 - r$, $p_2 = 0$, $p_3 = 0$, and $p_4 = 0$ [12], where p_1 decides the rate of achieving synchronization. p_1 is selected as $p_1 = -30 < 1 - r$ for the current simulation. For further reduction in coupling complexity, we choose the driver as identical to the response except $r + \Delta r = 38$. The mismatch is thereby limited to $\Delta r = 10$, when $\Delta\sigma = 0$ and $\Delta b = 0$. Numerical results of the coupled Lorenz system (5) and (6) are shown in Fig. 1. The response variables (x_i, $i = 1, 2, 3$) as solid lines and twice the driver variables (y_i) as dashed lines are plotted in the upper row. All of the time series are identical in amplitude but opposite in phase. This rules out the earlier claim [8–10] that (x_1, y_1) and (x_2, y_2) can attain only AS while (x_3, y_3) can be in CS. A plot of $E = (x_1 + 2y_1)$ in the lower left panel shows a constant value at zero with time that confirms an amplification of the driver by a factor of 2 as expected for $\alpha = -2$. The response attractor in Fig. 2(b) is a larger and inverted version of the driver in Fig. 2(a). The amplification is also realizable in the CS regime by simply taking $\alpha = 2$ as shown in the lower right plot of Fig. 1. Similarly, attenuation can be observed by taking $0 < |\alpha| < 1$.

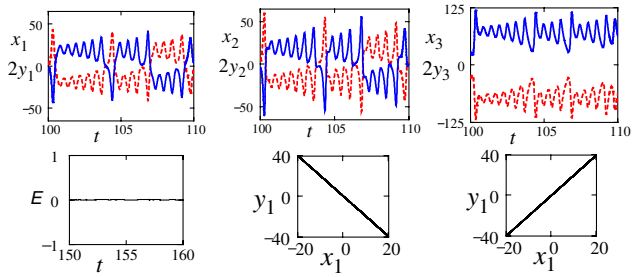

FIG. 1 (color online). Coupled Lorenz system. Response: $r = 28$, $\sigma = 10$, $b = 8/3$, driver identical except $\Delta r = 10$; $\varepsilon = 1$. Upper row: Time series of $(x_1, 2y_1)$ at left, $(x_2, 2y_2)$ at middle, and $(x_3, 2y_3)$ at right. Lower row: Plot of E at left, plots of y_1 vs x_1 confirm AS ($\alpha = -2$) at middle, CS ($\alpha = 2$) at right.

We consider the Rössler system as a second example:

$$\dot{x}_1 = -\omega x_2 - x_3; \quad \dot{x}_2 = x_1 + bx_2; \quad \dot{x}_3 = c + x_3(x_1 - d). \tag{7}$$

The driver oscillator with a mismatch is defined by

$$\dot{y}_1 = -\omega y_2 - y_3 - \Delta\omega y_2; \qquad \dot{y}_2 = y_1 + by_2 + \Delta by_2; \qquad \dot{y}_3 = c + y_3(y_1 - d) + \Delta c - \Delta dy_3, \tag{8}$$

where $\Delta\omega$, Δb, Δc, and Δd are the mismatches.

After coupling, the response Rössler is obtained as

$$\begin{aligned} \dot{x}_1 &= -\omega x_2 - x_3 - \alpha\Delta\omega y_2; \\ \dot{x}_2 &= x_1 + bx_2 + \alpha\Delta by_2; \\ \dot{x}_3 &= c + x_3(x_1 - d) + \alpha\Delta c + \alpha\Delta dy_3 + \alpha(1 - \alpha)y_1y_3 \\ &\quad + (p_1 - \alpha y_3)(x_1 - \alpha y_1) + (p_2 - \alpha y_1)(x_3 - \alpha y_3). \end{aligned} \tag{9}$$

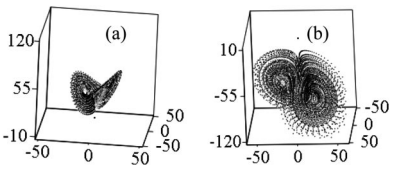

FIG. 2. Lorenz attractor ($\alpha = -2$): (a) 3D driver and (b) amplified and inverted response. Similar axes are drawn in the same scale.

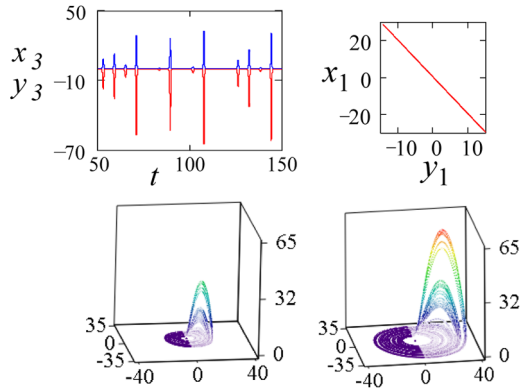

FIG. 3 (color online). Coupled Rössler system. Response: $\omega = 1$, $b = 0.15$, $c = 0.2$, $d = 10$; driver identical except $\Delta\omega = 0.15$. Upper row: Time series at left panel, y_3 above, x_3 below at left; response is amplified and antiphase to the driver for $\alpha = -2$; plot x_1 vs y_1 at right panel. Lower row: 3D attractors of driver (y_i) at left, of response ($-x_i$, $i = 1, 2, 3$) at right; similar axes kept in same scale. $H = |0\ -1\ -1; 1\ b\ 0; p_1\ 0\ p_2|^T$.

The parameters in H are designed as $p_1 = 1$ and $p_2 = 9$ to establish stable synchronization. Figure 3 shows the numerical results that confirm antiphase between the response variable x_3 and driver variable y_3. This is also true for the other state variables. The 3D trajectories in the lower row confirm amplification of the driver in the response. The response variables are inverted in the 3D plot for visual resemblance with the driver.

Next, we present a Sprott system [14] with a single quadratic nonlinearity as given by

$$\dot{x}_1 = -ax_2; \qquad \dot{x}_2 = x_1 + x_3; \qquad \dot{x}_3 = x_1 + {x_2}^2 - x_3. \tag{10}$$

Another mismatch Sprott system is taken as a driver

$$\dot{y}_1 = -ay_2 - \Delta a y_2; \quad \dot{y}_2 = y_1 + y_3; \quad \dot{y}_3 = y_1 + {y_2}^2 - y_3. \tag{11}$$

After coupling, the response system (10) becomes

$$\dot{x}_1 = -ax_2 - \alpha\Delta a(1/\varepsilon)y_2; \qquad \dot{x}_2 = x_1 + x_3;$$
$$\dot{x}_3 = x_1 + {x_2}^2 - x_3 + \alpha(1-\alpha){y_2}^2 + (p - 2\alpha y_2)(x_2 - \alpha y_2). \tag{12}$$

ε is the tuning parameter and taken as unity for the current simulation. The driver and the response are chaotic before coupling for ($a = 0.225$, $\Delta a = 0.025$). With a choice of $p = -1$, we find AS and amplification for $\alpha = -2$ as shown in Fig. 4. In the upper row, the middle 2D attractor is the amplified and inverted response of the driver attractor in the left; the plot of y_1 vs x_1 in the right confirms AS. The time series of the driver and the response, in the lower left panel, are clearly at opposite phase although their amplitudes are different. A measure of $E = (x_1 + 2y_1)$ maintains a zero value after the initial transients as shown in lower right panel. This confirms an amplification of the driver attractor in the response by a factor of 2.

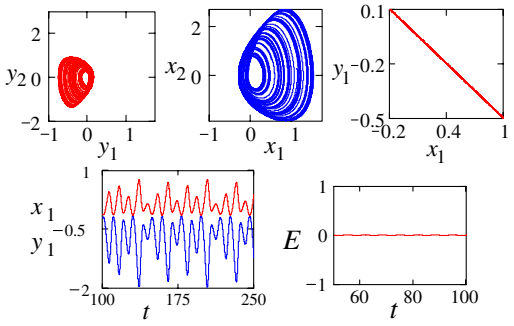

FIG. 4 (color online). Coupled Sprott system. Upper row: 2D driver at left and its response at middle; similar axes kept in the same scale; y_1 vs x_1 plot at right. Lower row: Time series at left panel, y_1 above, x_1 below, and plot of E with time at right. $H = [0\ -a\ 0; 1\ 0\ 1; 1\ p\ -1]^T$.

Now we attempt to understand the effect of the additional linear coupling terms on the stability of synchronization by tuning ε. The ε is tuned from both sides of the critical value ($\varepsilon = \varepsilon_c = 1$), higher and lower. The error between the driver and the response is then estimated by using a similarity measure [6]

$$\delta = \frac{\langle [x_1(t) - \alpha y_1(t-\tau)]^2 \rangle}{[\langle x_1(t)^2 \rangle \langle y_1(t)^2 \rangle]^{1/2}}. \tag{13}$$

A global minimum of $\delta = \delta_{\min} = 0$ stands for stable synchronization either CS or AS depending on the sign of α values (delay $\tau = 0$ for CS or AS). For the Sprott system, ε is varied from 0.5 to 1.5 to obtain $\delta_{\min} = 0$ at $\varepsilon = \varepsilon_c$ for a mismatch, $\Delta a = 0.025$, and the corresponding $\ln(\delta)$ vs $(\varepsilon - \varepsilon_c)$ plot is shown in Fig. 5(a). A sharp dipping into the minimum is observed at the critical value $\varepsilon_c = 1$ when a stable synchronization is attained. Effectively, ε acts as a strength of the additional linear coupling. Any compromise with the strength of this coupling term will induce degradation of synchrony. The process of transition to synchrony is found to be independent of the system and the type of mismatch, as it is shown to repeat in Fig. 5(b) for a coupled Lorenz system where ε

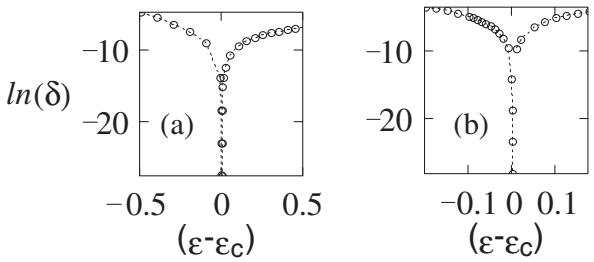

FIG. 5. Transition to synchrony in (a) a coupled Sprott system and (b) a Lorenz system. Open circles are for numerical data points.

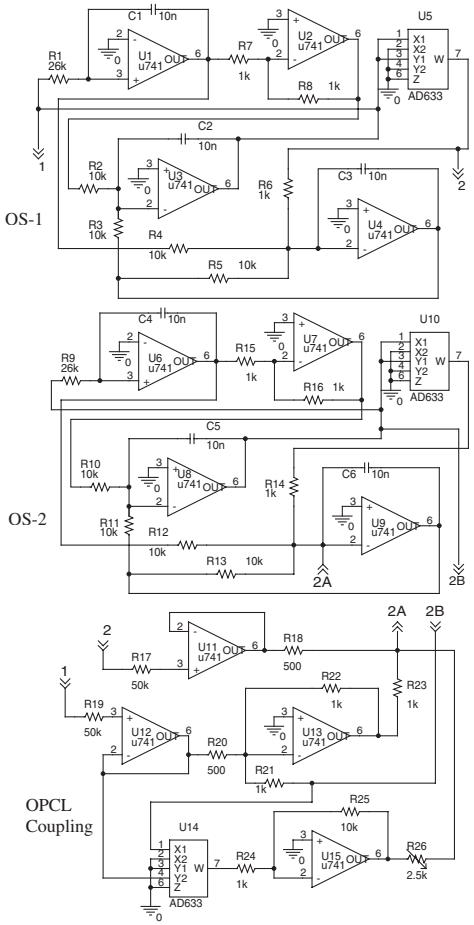

FIG. 6. Coupled Sprott circuit: OS-1 connects OS-2 via OPCL coupling; component values (1% tolerance) are noted.

is tuned from 0.8 to 1.2. However, we need further studies for a complete understanding of this transition.

Finally, we present a physical realization of the coupled Spott system (11) and (12). Figure 6 shows the coupled circuit. The Op-Amp U1-U5 (U6-U10) with resistances R_1-R_8 (R_9-R_{16}) and capacitances C_1-C_3 (C_4-C_6) represent the driver OS-1 (response OS-2). The OPCL coupling is designed using U11-U15. The continuity between the three parts of the circuit, OS-1, OS-2, and OPCL coupling is maintained via the terminals (1-1, 2-2 and 2A-2A, 2B-2B). Measurements of the driver and the response variables [analogs of y_1 and x_1 in Eqs. (11) and (12)] are made at the outputs of U1 and U6, respectively, using a 4-channel digital oscilloscope (Yokogawa, DL9140, 1 GHZ, 5 gigasamples/s). Experimental results shown in Fig. 7 are in good agreement with the numerical results in Fig. 4.

To summarize, the OPCL coupling ensures robust synchronization in mismatch chaotic oscillators. The AS is realized without any restriction on the symmetry class of a system. Robust amplification is also possible using this coupling. The physical realization of the coupling is not difficult as shown in a Sprott circuit. We have also checked that the coupling scheme can realize stable synchronization in the presence of noise.

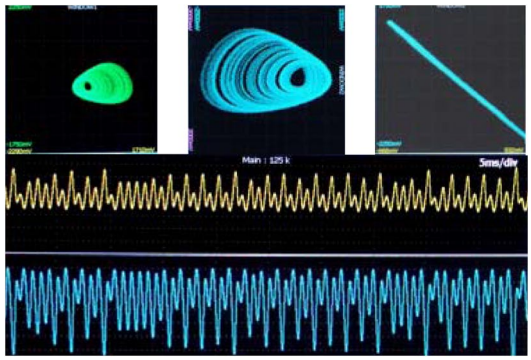

FIG. 7 (color online). Oscilloscope picture: 2D attractors in upper row, driver at left, amplified response at middle, axes in the same scales; output voltages of U1 vs U6 at right. Middle row: Driver time series. Lower row: Response time series.

The Ministry of Science & Technology, India and the Ministry of Education & Research, Romania supported (Grant No. INT/ROM/R-10/03) this work. S. K. D. acknowledges support (Grant No. SR/S2/HEP-03/05) by the DST, India.

*Corresponding author.
skdana@iicb.res.in

[1] A. Argyris *et al.*, Nature (London) **438**, 343 (2005).
[2] P. Mohanty, Nature (London) **437**, 325 (2005).
[3] F. Hoppensteadt and E. Izhikevich, U.S. Patent No. 6957204 (2005).
[4] P. J. Uhlhaas and W. Singer, Neuron **52**, 155 (2006).
[5] L. Pecora and T. Carroll, Phys. Rev. Lett. **64**, 821 (1990).
[6] A. Pikovsky, M. Roseblum, and J. Kurths, *Synchronization: A Universal Concept in Nonlinear Sciences* (Cambridge University Press, Cambridge, England, 2001).
[7] S. C. Venkataramani, B. Hunt, and E. Ott, Phys. Rev. Lett. **77**, 5361 (1996); V. Astakov *et al.*, Phys. Rev. E **58**, 5620 (1998); R. L. Viana *et al.*, Physica (Amsterdam) **206D**, 94 (2005).
[8] L.-Y. Cao and Y.-C. Lai, Phys. Rev. E **58**, 382 (1998); V. Astakov *et al.*, Int. J. Bifurcation Chaos Appl. Sci. Eng. **10**, 849 (2000).
[9] W. Liu *et al.*, Phys. Rev. E **73**, 057203 (2006); C.-M. Kim *et al.*, Phys. Lett. A **320**, 39 (2003).
[10] V. Belykh, I. Belykh, and M. Hasler, Phys. Rev. E **62**, 6332 (2000).
[11] I. Wedekind and U. Parlitz, Phys. Rev. E **66**, 026218 (2002).
[12] E. A. Jackson and I. Grosu, Physica (Amsterdam) **85D**, 1 (1995); I. Grosu, Phys. Rev. E **56**, 3709 (1997); I. Grosu, Int. J. Bifurcation Chaos Appl. Sci. Eng. **17**, 3519 (2007).
[13] J. M. Gonzalez-Miranda, Phys. Rev. E **57**, 7321 (1998).
[14] J. C. Sprott, Phys. Rev. E **50**, R647 (1994).
[15] C. Li, W. Sun, and J. Kurths, Phys. Rev. E **76**, 046204 (2007).
[16] I. Grosu, E. Padmanaban, and S. K. Dana (to be published).